Drug Design, Development and Therapy

Dovepress
Taylor & Francis Group

Open Access Full Text Article

ORIGINAL RESEARCH

Puerarin Ameliorates the Ferroptosis in Diabetic Liver Injure Through the JAK2/STAT3 Pathway Inhibition Based on Network Pharmacology and Experimental Validation

Xiaoxu Fan[1], Shuangqiao Liu[1], Jing Yu[2], Jian Hua[1], Yingtong Feng[1], Zhen Wang[1], Yiwei Shen[1], Wei Lan[2], Jingxia Wang[1]

[1]School of Traditional Chinese Medicine, Beijing University of Chinese Medicine, Beijing, People's Republic of China; [2]School of Traditional Chinese Medicine, Xinjiang Medical University, Urumqi, People's Republic of China

Correspondence: Jingxia Wang, School of Traditional Chinese Medicine, Beijing University of Chinese Medicine, Beijing, People's Republic of China, Email 601435@bucm.edu.cn; Wei Lan, School of Traditional Chinese Medicine, Xinjiang Medical University, Urumqi, People's Republic of China, Email lanwei516@sina.com

Background: Diabetic liver injury (DLI) is a common complication of diabetes mellitus (DM), which seriously endangers the health of diabetic patients. Puerarin, the main active component of *Pueraria lobata*, has shown positive effects in lowering blood glucose and lipids, resisting oxidative stress, and protecting the liver. However, the mechanism of protective effect of Puerarin on DLI remains unclear.

Methods: Various databases were used to screen for targets of Puerarin, ferroptosis and DLI. Protein-protein interaction (PPI) network and Kyoto Encyclopedia of Genes and Genomes (KEGG) enrichment analysis were used to predict key targets and pathways. Molecular docking was used to predict the interactions between Puerarin and core targets. KK/Upj-Ay/J (KKAy) mice and high glucose (HG)-induced AML12 cells were used to study the protective effect of Puerarin on DLI. The molecular mechanisms by which Puerarin acts were further verified by in vivo and in vitro experiments.

Results: KEGG analysis indicated that the JAK/STAT pathway might be related to the anti-DLI effect of Puerarin. Molecular docking revealed that Puerarin has good affinity for JAK2 and STAT3. In vivo, Puerarin (80 mg/kg) reduced body weight, blood glucose, blood lipids and liver function in KKAy mice fed a high-sugar, high-fat diet. Puerarin also ameliorated hepatic pathological changes and inflammatory responses, and attenuated oxidative stress and iron overload in KKAy mice. Western blotting results showed that Puerarin could regulate the expression of proteins related to JAK2/STAT3 pathway and ferroptosis pathway. In vitro, Puerarin (25, 50, 100 μM) increased cell viability and decreased steatosis and liver function indexes in AML12 cells induced by HG (30 mm) to varying degrees. More importantly, AG490 blocker experiments showed that the regulation of ferroptosis process by Puerarin was dependent on the JAK2/STAT3 pathway.

Conclusion: In conclusion, this study revealed Puerarin may regulate the ferroptosis process by inhibiting the JAK2/STAT3 pathway for the treatment of DLI.

Keywords: puerarin, diabetic liver injury, ferroptosis, JAK2/STAT3 pathway, network pharmacology

Introduction

Diabetes, a common chronic metabolic disease, has become a serious global health problem affecting people of all ages. Diabetes is a disease characterised by elevated blood glucose levels caused by inadequate insulin secretion or insulin resistance. Type 2 diabetes is predominant, accounting for more than 90% of patients.[1] Over time, diabetes may damage the liver, kidneys, blood vessels, eyes, and nerves.[2] Among these, the liver is an important metabolic centre of the body and one of the main target organs involved in diabetic complications. Diabetic liver injury (DLI) is a series of liver

Received: 19 August 2024
Accepted: 29 January 2025
Published: 1 February 2025

Graphical Abstract

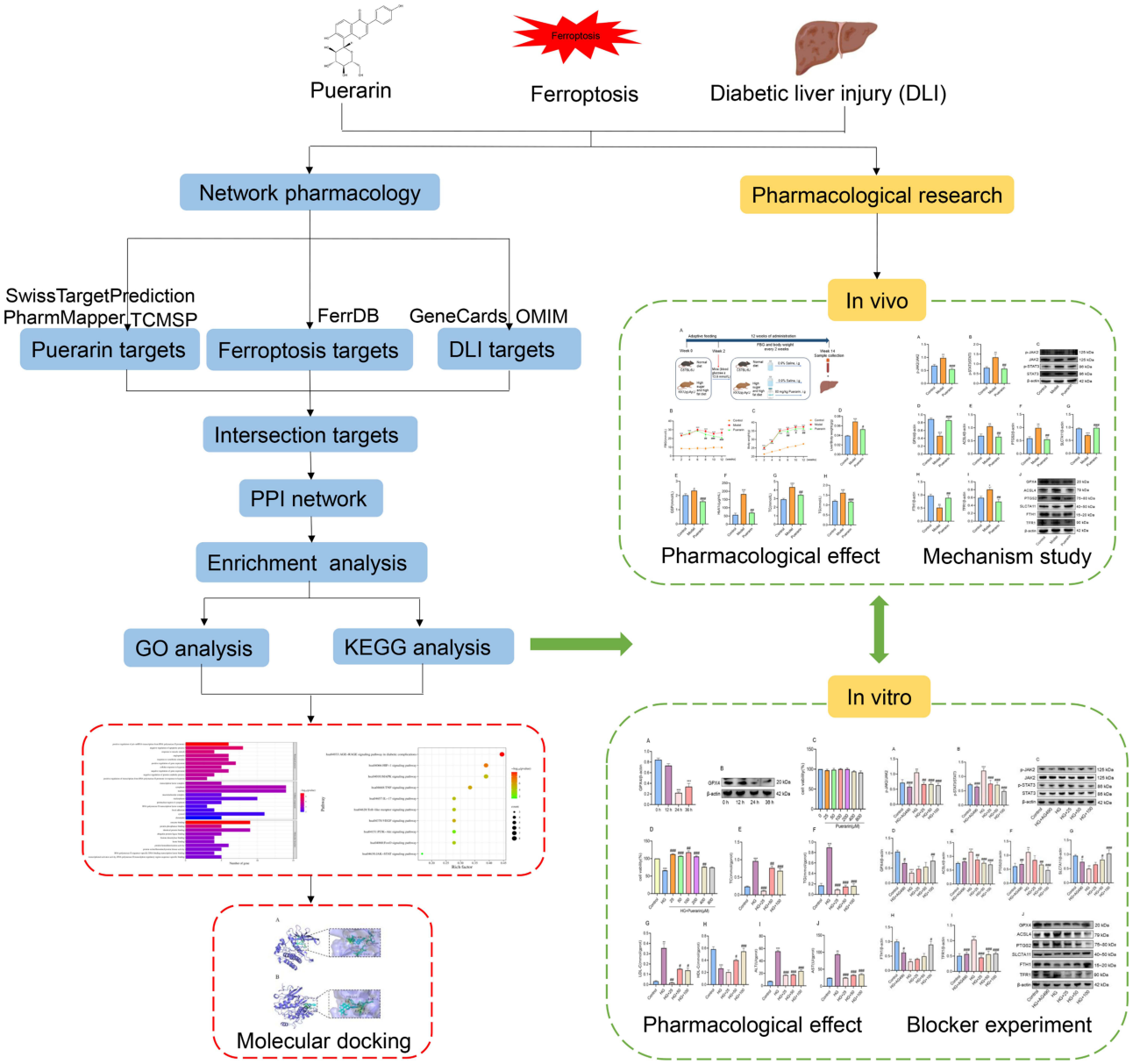

diseases including altered liver function, non-alcoholic fatty liver disease (NAFLD), cirrhosis, and liver failure caused by diabetes-related metabolic disorders.[3] Oral chemical hypoglycemic drugs have various degrees of damaging effects on the liver. Therefore, it is becoming increasingly important to urgently develop safer and more effective drugs for the treatment of DLI and to further enhance research on the pathogenesis of DLI.

Puerarin, an isoflavonoid compound, is one of the main active ingredients extracted from the tuberous roots of *Pueraria lobata*. Puerarin has biological activities such as anti-tumor, anti-inflammatory, antioxidant, immune enhancement and cardiovascular protection.[4–7] In recent years, Puerarin has a variety of medical uses and has been widely used in the treatment of cancer, fatty liver, cardiovascular and cerebrovascular diseases, diabetes and diabetic complications.[8,9] It was shown that Puerarin significantly improved hepatic steatosis, reduced inflammatory response and improved leptin

signaling through the JAK2/STAT3 pathway in NAFLD rats.[10] Steatohepatitis plays a key role in the process leading to liver fibrosis and cirrhosis.[11] Puerarin was found to alleviate steatohepatitis. Specifically, Puerarin extract was able to activate the AMPK/PPARα pathway and decrease the expression of SREBP-1 and FAS proteins, thereby inhibiting hepatic lipid deposition and increasing the antioxidant capacity of the liver.[12] In addition, Puerarin inhibited hepatic gluconeogenesis in diabetic rats and HepG2 cells through activation of the PI3K/Akt/FOXO1 pathway.[13] The above studies confirmed that Puerarin has great potential in the treatment of DLI, but the underlying molecular mechanisms still need to be further explored.

Ferroptosis is a mode of cell death driven by iron-dependent phospholipid peroxidation. The mechanism of ferroptosis is mainly related to iron metabolism disorders, lipid peroxide accumulation, and imbalance of amino acid antioxidant system.[14] Studies have shown that ferroptosis is one of the pathogenic mechanisms in numerous liver diseases, such as liver injury, non-alcoholic steatohepatitis, liver fibrosis, cirrhosis and hepatocellular carcinoma.[15–17] The study reported that ferroptosis was involved in the process of acetaminophen (APAP)-induced acute liver injury. Specifically, hepatic iron deposition enhanced APAP-induced toxicity, oxidative stress and mitochondrial dysfunction in primary mouse hepatocytes (PMHs).[18] Ferroptosis has also been found to play a key regulatory role in the development of NAFLD. Herbal medicines can alleviate high-fat diet-induced NAFLD by inhibiting ferroptosis in vivo and in vitro.[19] Research has also proven that targeting ferroptosis is a promising strategy for the treatment of DLI. More importantly, Puerarin was found to be able to ameliorate fatty liver disease associated with metabolic disorders by inhibiting ferroptosis and inflammation through the SIRT1/Nrf2 signaling pathway.[20] In addition, numerous scholars have demonstrated that Puerarin is able to regulate iron homeostasis and inhibit iron overload, thereby inhibiting cellular iron death.[21] However, the therapeutic effect of Puerarin on high glucose and high fat diet-induced DLI in KKAy mice and the mechanism of ferroptosis have not been elucidated.

The JAK/STAT pathway is activated in DM, of which the JAK2/STAT3 subtype is the most widely and intensively studied. The JAK2/STAT3 pathway, widely present in all types of tissues and cells of the body, is involved in biological processes such as cell growth, differentiation, apoptosis, and immunomodulation.[22] The JAK2/STAT3 pathway can mediate inflammation, oxidative stress, cell proliferation and fibrosis.[23] Studies have shown that the JAK2/STAT3 pathway is involved in the lipid metabolism of cholesterol, triglycerides, and fatty acids in the body. Modulation of the JAK2/STAT3 pathway improved hepatic lipid metabolism and inflammation in high-fat diet-induced obese mice.[24] It was also reported that the JAK2/STAT3 pathway could mediate tissue repair and adipogenesis in the body to regulate hyperlipidaemia.[25] Besides, inhibition of the JAK2/STAT3 and JAK2/p38/NF-κB pathways was able to exert hepatoprotective effects on D-galactose-induced liver injury in mice.[26] In conclusion, the JAK2/STAT3 pathway is a promising target for the treatment of liver diseases. More importantly, in the inflammatory microenvironment, the JAK2/STAT3 pathway is closely related to ferroptosis, and both of them interact with each other.[27] Activation of the JAK2/STAT3 pathway can regulate the expression of genes related to iron metabolism, which further affects the accumulation of iron ions and the occurrence of ferroptosis. In turn, the accumulation of iron ions can activate the JAK2/STAT3 pathway, further enhancing the inflammatory response.[28] Therefore, given that DLI is a classic inflammatory disease, this study hypothesized that Puerarin might ameliorate DLI by inhibiting ferroptosis through regulating the JAK2/STAT3 pathway.

In this study, KKAy mouse model and HG-induced AML12 cell model were used to investigate the protective effect of Puerarin on DLI and its mechanism of action. In addition, our research aimed to determine the role of ferroptosis in DLI, elucidate the relationship between hepatic ferroptosis and the JAK2/STAT3 pathway via using AG490 (JAK2 inhibitor).

Materials and Methods

Drugs and Reagents

Puerarin (purity > 98%, B20446) and AG490 (purity > 99%, HY-12000) were purchased from Yuanye Biotechnology Co., Ltd (Shanghai, China) and MCE (NJ, USA), respectively. Glucose (1181302) was obtained from Sigma (Missouri, USA).

GSP (A037-1-1), HbA1c (H464-1-1), ALT (C009-2-1), AST (C010-2-1), TC (A111-1-1), TG (A110-1-1), LDL-C (A113-1-1), and HDL-C (A112-1-1) kits were provided by Jiancheng Biotechnology Co., Ltd (Nanjing, China). Oil red O staining kit was purchased from Solarbio Biotechnology Co., Ltd (Beijing, China). SOD (E-BC-K020-M), MDA (E-BC-K025-M), GSH (E-BC-K030-M), GSH-Px (E-BC-K096-M), total iron (E-BC-K772-M), and ferrous iron (E-BC-K773-M) colorimetric assay kits as well as IL-6 (E-MSEL-M0001) and TNF-α (E-MSEL-M0002) ELISA kits were provided by Elabscience Biotechnology Co., Ltd (Wuhan, China). BCA protein assay (KGP902) and CCK-8 (CK001) kits was purchased from Kaiji Biology (Jiangsu, China) and LABLEAD (Beijing, China), respectively. Reagents used for cell culture were purchased from VivaCell (Shanghai, China). Besides, the antibodies and their dilution ratios used in this study are as follows: anti-JAK2 (3230T, 1:1000), anti-STAT3 (4904S, 1:2000), anti-phospho-JAK2 (4406T, 1:1000), and anti-phospho-STAT3 (9145T, 1:2000) were purchased from Cell Signaling Technology (Danvers, MA, USA). Anti- NF-κB p65 (YT3108, 1:2000), anti-GPX4 (YN3047, 1:2000), anti-SLC7A11 (YT8130, 1:2000), anti-TFR1 (YT5374, 1:2000), anti-FTH1 (YT1692, 1:1000), and anti-ACSL4 (YT8070, 1:2000) were purchased from Immunoway (California, USA). Anti-phospho-NF-κB p65 (82,335-1-RR, 1:2000), anti-PTGS2 (12,375-1-AP, 1:1000), anti-β-actin (20536-1-AP, 1:5000), and HRP-conjugated affinipure goat anti-rabbit IgG (SA00001-2, 1:5000) were obtained from Proteintech (Chicago, USA).

Network Pharmacology Analysis

Collection of Puerarin and DLI Targets

Puerarin targets were searched through TCMSP (https://old.tcmsp-e.com/tcmsp.php), SwissTargetPrediction (http://swisstargetprediction.ch/), and PharmMapper databases (https://lilab-ecust.cn/pharmmapper/index.html). Puerarin targets were identified after merging the three databases and removing duplicate data. UniProt database (https://www.uniprot.org/) was used to uniformly transform Puerarin targets. Besides, disease targets were searched in GeneCards (https://www.genecards.org/) and OMIM databases (https://www.omim.org/) using "diabetic liver injury" as the key word. Similarly, the targets were standardised in the UniProt database (https://www.uniprot.org/).

Acquisition of Ferroptosis and Intersection Targets

Genes associated with ferroptosis, such as "Marker", "Suppressor", and "Driver", were retrieved from the FerrDB database (http://www.zhounan.org/ferrdb). Ferroptosis data from each module were downloaded. After merging, duplicate data were removed. The Venny 2.1 (https://bioinfogp.cnb.csic.es/tools/venny/) software was applied to obtain the intersection targets of Puerarin, DLI, and ferroptosis. The common targets of all three may be the key targets for Puerarin to treat disease by regulating ferroptosis.

PPI Network Construction, GO and KEGG Enrichment Analysis

The intersection targets were entered into the String database (https://string-db.org/cgi/input.pl) and exported as a tsv file with the organism type set to "homo sapiens" and confidence level > 0.9. This file was imported into Cytoscape 3.8.0 for PPI network mapping. Besides, the intersection targets were imported into the DAVID database (https://david.ncifcrf.gov/) for GO and KEGG enrichment analysis. Visualisation was performed through the microbiotics online platform (http://www.bioinformatics.com.cn).

Molecular Docking

The 3D structures of key target proteins, including JAK2 and STAT3, were downloaded in "PDB" format via the RSCB PDB database (http://www.rcsb.org). The 2D structure of Puerarin was downloaded from the PubChem database (https://pubchem.ncbi.nlm.nih.gov/) and imported into Chem3D software for conversion to MOL2 format. Target proteins and small molecules were removed water molecules, added full hydrogen, and automatically assigned charges using AutoDockTools 1.5.6 software, followed by molecular docking by AutoDock Vina. PyMoL 2.3.4 software was used to visualize the docking results.

Animals and Experimental Design

Male C57BL/6J and KKAy mice used in this study, 12-week-old, specific pathogen-free (SPF) grade, were purchased from Beijing HuaFuKang Biotechnology Co., Ltd., [Licence No. SCXK (Beijing) 2019–0008]. The study protocol was approved by the Institutional Animal Care and Use Committee of Beijing University of Chinese Medicine (Ethics Reference Number: BUCM-2022122601-4086). All animal experiments were performed by complying with the guidelines for the Protection and Use of Experimental Animals of the Ministry of Science and Technology of China. Mice with the random blood glucose ≥ 13.9 mmol/L identified as diabetic were selected and included in the experiment. Mice were given sufficient food and water during the experiments. The room temperature of the animal house was 20~24°C, relative humidity 60~70%, and a typical 12-hour light-dark cycle.

After 2 weeks of adaptive feeding, KKAy mice were randomly divided into two groups according to blood glucose and body weight: model group (KKAy) and Puerarin group (KKAy + 80 mg/kg, i.g.) with 8 mice in each group. The other 8 C57BL/6J mice were the control group. All mice, except the control group, were fed high sugar and high fat feed. The control and model groups were given equal volumes of 0.9% saline. The Puerarin group was administered 80 mg/kg Puerarin by gavage. The dose of Puerarin administered was obtained from the appropriate literature.[29] Mice were administered the treatment for 12 consecutive weeks.

Sample Collection and Biochemical Analysis

During the experiment, the fasting blood glucose and body weight of mice were measured every 2 weeks. After 12 weeks, blood was taken to detect serum FBG, HbA1c, GSP, TC, TG, LDL-C, HDL-C, ALT, and AST levels according to the instructions of the kits. Livers were taken and tested for relevant indicators. The liver index was calculated using the formula:

$$\text{Liver index} = \text{liver weight (g)} / \text{Body weight (g)}$$

Assessment of Liver Iron, SOD, MDA, GSH, and GSH-Px Levels

Liver iron, SOD, MDA, GSH, and GSH-Px levels were detected using colorimetric assay according to the instructions of the corresponding kits.

Elisa

Liver IL-6 and TNF-α levels were measured by enzyme-linked immunosorbent assay according to the manufacturer's instructions.

Histological Analysis

Fresh liver tissue was removed and fixed with paraformaldehyde. After 24 h, the tissue was dehydrated and embedded in paraffin. Liver tissue was cut into 4 μm sections for hematoxylin-eosin (HE) staining. Liver structure was observed using the microscope.

Cell Culture and Treatment

AML12 cells, purchased from Prolife Biotechnology Co., Ltd (No. CL-0602; Wuhan, China), were cultured in Dulbecco's modified Eagle medium/nutrient mixture F-12 (DMEM/F12) containing 10% fetal bovine serum with 1% penicillin-streptomycin. Cells were cultured in an incubator with 37°C and 5% CO_2. The medium was changed every 2 days. When the cell density reached 80~90%, 0.25% trypsin-EDTA was used to digest cells and passaged in a 1:3 ratio. AML12 cells were epithelial cell-like and grow in a polygonal adherent shape.

Cell Viability Assay

According to the previous study, a model of DLI was established with 30 mm HG intervention.[30] The Cell Counting Kit-8 (CCK-8) was used to detect Puerarin toxicity and screen for optimal Puerarin concentration. AML12 cells were plated in 96-well plates at a density of 5×10^4 cells/mL. After 24 h of pre-culture, Puerarin at concentrations of 25, 50, 100, 200,

400 and 800 μM was administered to control cells and modeled cells, respectively. After 24 h of dosing treatment, 10 μL CCK-8 solution was added to each well and incubated at 37°C without light for 1 h. Subsequently, the absorbance at 450 nm was determined by a microplate reader (Multiskan FC). Puerarin was solubilized with DMSO and required ultrasonic. Glucose was dissolved with DMEM/F12. Puerarin administration concentration and time were determined with reference to relevant literature.[20]

Oil Red O Staining

Fresh liver tissue was embedded in OCT, cut into 10 μm sections, and stained with Oil red O reagent. For Oil red O staining of AML12 cells, AML12 cells were grown in 6-well plates and fixed with 4% paraformaldehyde for 15 min, followed by staining. The distribution of liver lipid droplets was observed using microscope.

Quantitative Lipid Analysis and Liver Function Determination

Liver tissue and cell homogenates were prepared by adding saline. Homogenate protein concentration was determined using a BCA kit. The levels of TC, TG, LDL-C, HDL-C, ALT, and AST in the homogenates were detected according to the kit instructions.

JAK2 Blocking Experiment

The blocker experiments were divided into six groups: control, model (high-glucose, HG), AG490 (HG + 50 μM AG490), and Puerarin (HG + 25, 50, and 100 μM Puerarin) groups. AML12 cells were cultured at a density of 1×10^5 cells/mL in 6-well plates. After pre-culture for 24 h, the remaining groups, except the control group, were modelled with 30 mm HG for 24 h. Next, cells in the Puerarin and AG490 groups were treated with 25, 50, 100 μM of Puerarin and 50 μM of AG490 for 24 h, respectively. Subsequently, the expression of the relevant proteins was determined using Western blotting. Puerarin and AG490 were solubilised with DMSO and diluted to the corresponding concentrations with DMEM/F12. The AG490 blocker dose has been reported in several studies.[31,32]

Western Blotting

Liver tissue and AML cells were lysed with RIPA buffer containing protease- and phosphatase inhibitors and supernatants were collected. Protein concentration was determined using a BCA kit. Then, 40 μg protein was separated by sodium dodecyl sulfate-polyacrylamide gel electrophoresis (SDS-PAGE) at 80 V for 2 h and transferred to PVDF membranes at 300 mA for 1 h. After blocking with 5% skim milk for 2 h, the membranes were incubated with primary antibodies overnight at 4 °C. On the following day, the membranes were incubated with secondary antibodies for 1 h. The membranes were scanned and analysed using a gel imaging system. The relative expression of target protein was calculated as the ratio of target protein to β-actin bands.

Statistical Analysis

The experimental data are presented as the mean ± standard deviation (SD). Statistical analyses and graphing were performed using SPSS 20 and GraphPad Prism 8. Differences between groups were compared using one-way ANOVA followed by LSD post hoc tests. $P < 0.05$ was considered a statistically significant difference.

Results

Investigation of the Mechanism of Puerarin Against DLI by Network Pharmacology and Molecular Docking Techniques

Puerarin, Ferroptosis, and DLI Targets Collection and Acquisition of Intersecting Targets

The 2D structure of Puerarin is shown in Figure 1A. A total of 269 drug targets were obtained using TCMSP, SwissTargetPrediction, and PharmMapper databases. 335 ferroptosis-related genes were obtained through the FerrDB database. Disease targets were collected through GeneCards and OMIM databases, and a total of 1217 targets were

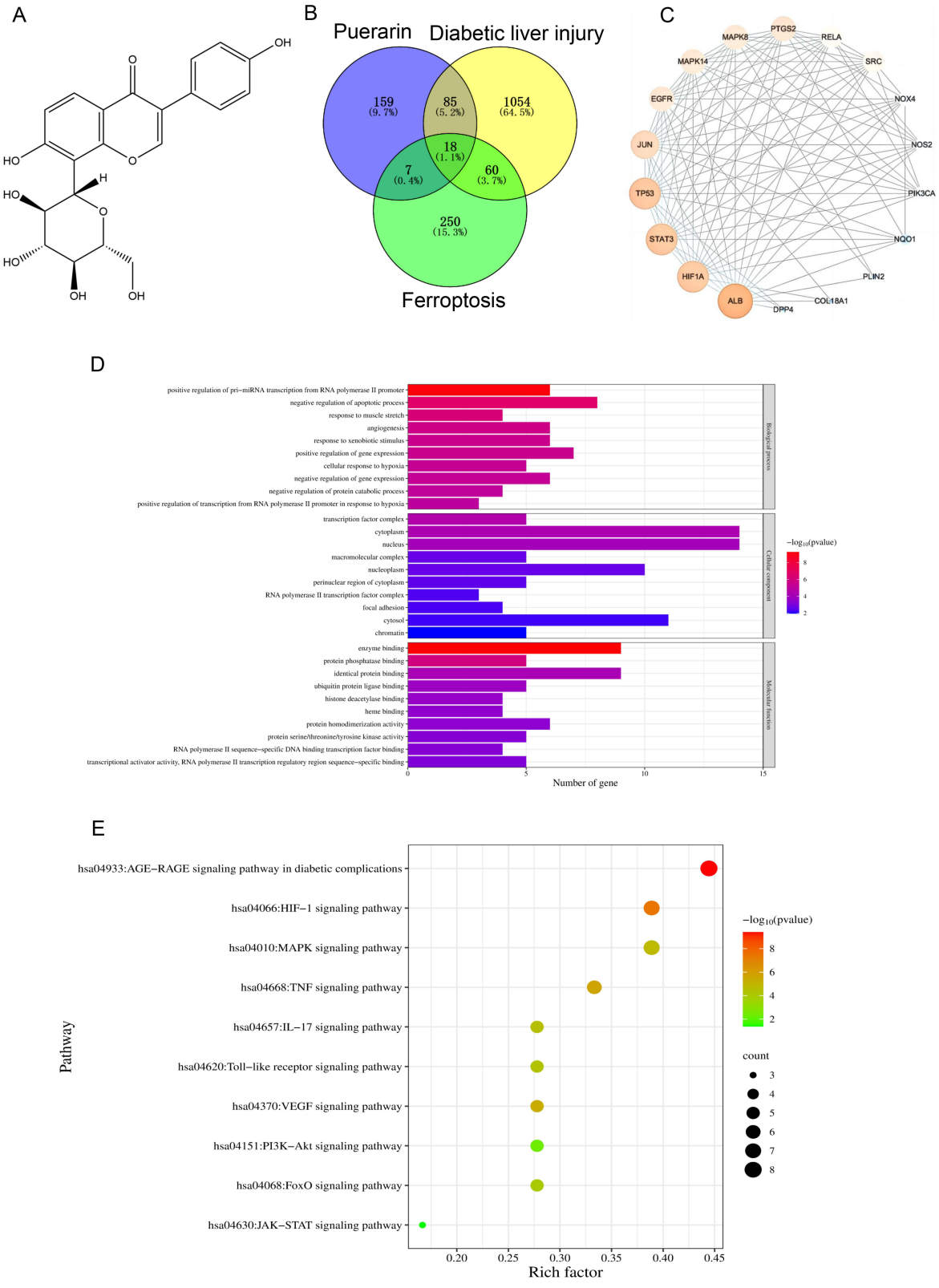

Figure 1 Investigation of the mechanism of Puerarin against DLI by network pharmacology. (**A**) Structure of Puerarin. (**B**) Intersection targets of Puerarin, ferroptosis, and DLI. (**C**) The PPI network of the intersection targets. (**D** and **E**) GO and KEGG enrichment analysis results.

https://doi.org/10.2147/DDDT.S487496

obtained after aggregation and de-duplication. 18 common targets were obtained by taking the intersection of Puerarin, DLI and ferroptosis targets, as shown in Figure 1B.

PPI Network Analysis

As shown in Figure 1C, the PPI network has 18 nodes and 97 edges. Nodes indicate target proteins, and its size and color indicate the intensity of action (ie, degree), with the color increasing from blue to orange, and the intensity of action increasing sequentially. Connections between nodes represent interactions between target proteins. The top five targets in terms of degree value were ALB, HIF1A, STAT3, TP53, and JUN, which predicted that these targets might be the key targets of Puerarin for the treatment of DLI via the ferroptosis pathway.

GO and KEGG Enrichment Analysis results

GO enrichment analyses yielded 149, 21, and 41 entries in biological processes (BP), cellular components (CC), and molecular functions (MF), respectively. The top 10 entries for each aspect were taken to make a visual bar chart based on $P < 0.05$. GO enrichment results showed that BP was mainly involved in the negative regulation of apoptotic process, angiogenesis, positive regulation of gene expression, and cellular response to hypoxia. CC showed that they were mainly present in the transcription factor complex, cytoplasm, nucleus, and macromolecular complex. In terms of MF, it plays a role in the enzyme binding, protein phosphatase binding, ubiquitin-protein ligase binding, and heme binding, as shown in Figure 1D.

KEGG pathway analysis enriched a total of 105 pathways. Non-signaling pathways were excluded and bubble plot was drawn based on entries with $P < 0.05$. KEGG enrichment analysis showed that common genes were mainly involved in JAK-STAT signaling pathway, AGE-RAGE signaling pathway, HIF-1 signaling pathway, TNF signaling pathway, and MAPK signaling pathway, as shown in Figure 1E. The higher the "Rich factor", the higher the enrichment. The results suggest that Puerarin may treat DLI through the above pathways.

Molecular Docking Results

It is generally accepted that the lower the ligand-receptor binding energy, the easier it is to dock successfully. The binding energies between target protein receptors (JAK2, STAT3) and a small molecule ligand (Puerarin) were −12.78 and −8.71 kcal/mol, respectively. The binding energies were all less than −5 kcal/mol, indicating high binding viability and stable docking. Puerarin can form hydrogen bonds with active sites, ASN-678, SER-698, GLN-626, LYS-581, and VAL-629, of the JAK2 gene encoding protein (PDB:8B8N). Furthermore, it can form hydrogen bonds with active sites, ASN-73, TYR-122, and GLN-123, of the STAT3 gene encoding protein (PDB: 5AX3). The molecular docking schematic is shown in Figure 2A and B.

Effects of Puerarin on Physical and Biochemical Markers in Mice with DLI

Initially, the therapeutic effect of Puerarin on DLI mice was explored (Figure 3A). The present study determined the changes in FBG and body weight of mice during 12 weeks of administration. The results show that FBG of the model group was significantly higher than the control group at 2, 4, 6, 8, 10, and 12 weeks of administration, suggesting successful modelling of type 2 diabetes mellitus (T2DM). On the contrary, Puerarin group significantly reduced FBG of the model group after 8 weeks of administration (Figure 3B). From the results of body weight monitoring, body weight was significantly higher in the model and Puerarin groups than in the control group, and Puerarin markedly decreased body weight of the model group from week 8 onwards (Figure 3C). The results also suggest that liver weight/body weight, GSP and HbA1c were significantly higher in the model group than in the control group, and these indices remarkably decreased after Puerarin treatment (Figure 3D-F). Upon further examination serum of lipid metabolites, we found that serum TC, TG and LDL-C levels were significantly higher and HDL-C was significantly lower in the model group of mice compared to the control group (Figure 3G-J). All the above indices were reversed when Puerarin intervened. In addition, while the model mice were observed to have a remarkably elevated ALT and AST levels, these two indices were significantly downregulated after Puerarin treatment (Figure 3K and L).

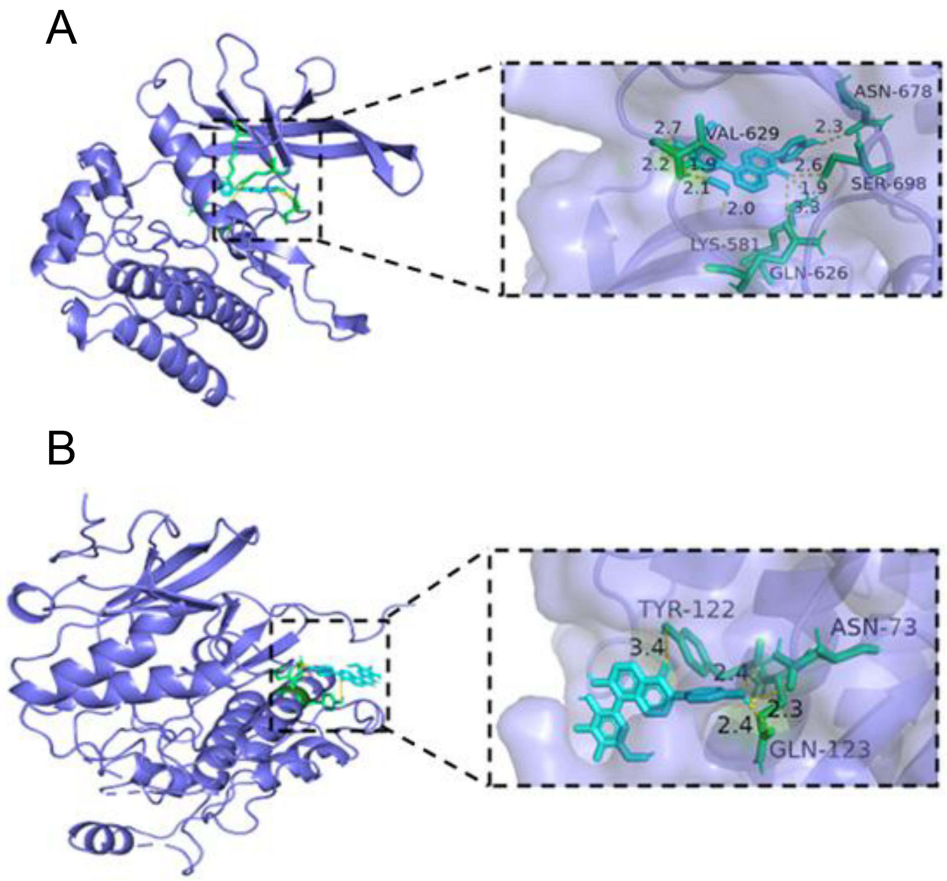

Figure 2 Results of molecular docking of Puerarin and key targets. (**A**) Molecular docking of Puerarin and JAK2. (**B**) Molecular docking of Puerarin and STAT3.

Effects of Puerarin on the Liver Pathology and Inflammatory Reaction in Mice with DLI

HE staining revealed disordered arrangement of the hepatic lobules, infiltration of inflammatory cells, appearance of vacuolar changes and steatosis in the model mice as compared to control group. The above pathological changes were significantly improved in the Puerarin group (Figure 4A). Furthermore, Oil red O staining observed significant lipid accumulation in liver in the model mice. However, less hepatic lipid droplets were observed after Puerarin treatment (Figure 4B). These data further demonstrated the protective effect of Puerarin.

Western blotting results showed that Puerarin markedly reduced p-NF-κB p65 protein expression in the model group (Figure 4C and D). Furthermore, ELISA results revealed that the levels of IL-1β and TNF-α in the Puerarin group were significantly lower than those in the model group (Figure 4E and F). These data suggest that the mechanism of action of Puerarin in ameliorating DLI may be related to the reduction of pro-inflammatory cytokine secretion via p-NF-κB p65 protein expression inhibition.

Effects of Puerarin on the Oxidative Stress, and Iron Overload in Mice with DLI

The purpose of this part was to explore the effect of Puerarin on liver oxidative stress levels and iron homeostasis in DLI mice. Lipid peroxidation and iron overload are vital in ferroptosis. The results showed that the levels of SOD, GSH, and GSH-Px of KKAy mice in the model group were significantly reduced compared to the control group, while there was a greatly rise in MDA levels, suggesting an increase in hepatic oxidative stress (Figure 4G-J). In contrast, the above indicators were reversed after Puerarin treatment. Besides, Fe^{2+} and total iron content increased significantly in the model group when compared to C57BL/6J mice, while Puerarin intervention notably inhibited iron overload and decreased iron content in the model group (Figure 4K and L). Collectively, Puerarin inhibited oxidative stress and iron overload in model mice.

https://doi.org/10.2147/DDDT.S487496

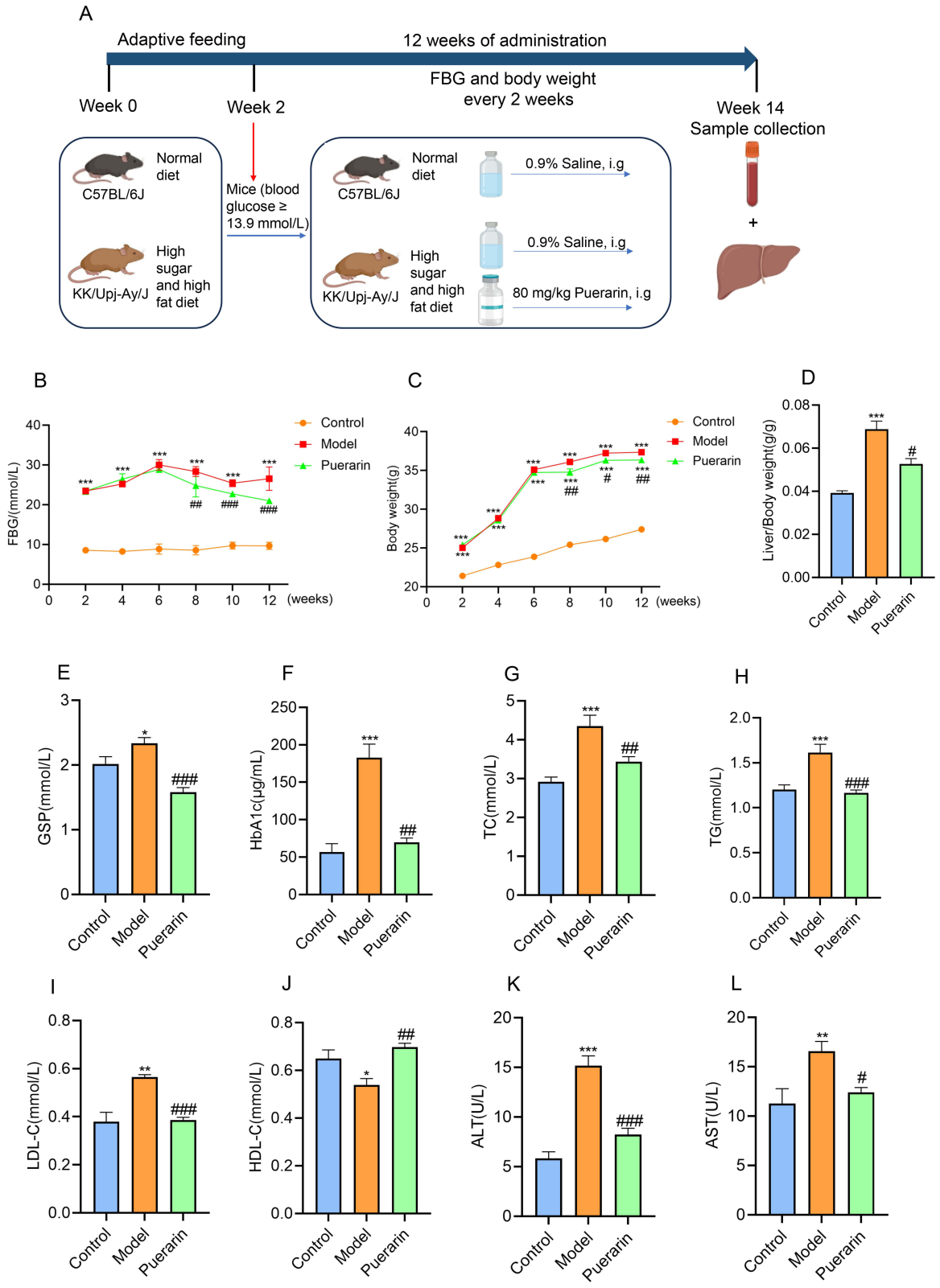

Figure 3 Effect of Puerarin on FBG, body weight, Liver index, blood lipids and liver function in mice with DLI. (**A**) Experimental procedure to evaluate the effects of Puerarin on DLI mice. (**B** and **C**) FBG and body weight every 2 weeks after the establishment of the T2DM model. (**D-F**) Liver index, serum GSP and HbA1c. (**G** and **J**) serum TC, TG, LDL-C, and HDL-C. (**K** and **L**) serum ALT and AST. Data represent means ± SD (n = 8); Statistical analysis tested by one-way ANOVA test. **P* < 0.05, ***P* < 0.01, ****P* < 0.001 vs control; $^{\#}P$ < 0.05, $^{\#\#}P$ < 0.01, $^{\#\#\#}P$ < 0.001 vs model.

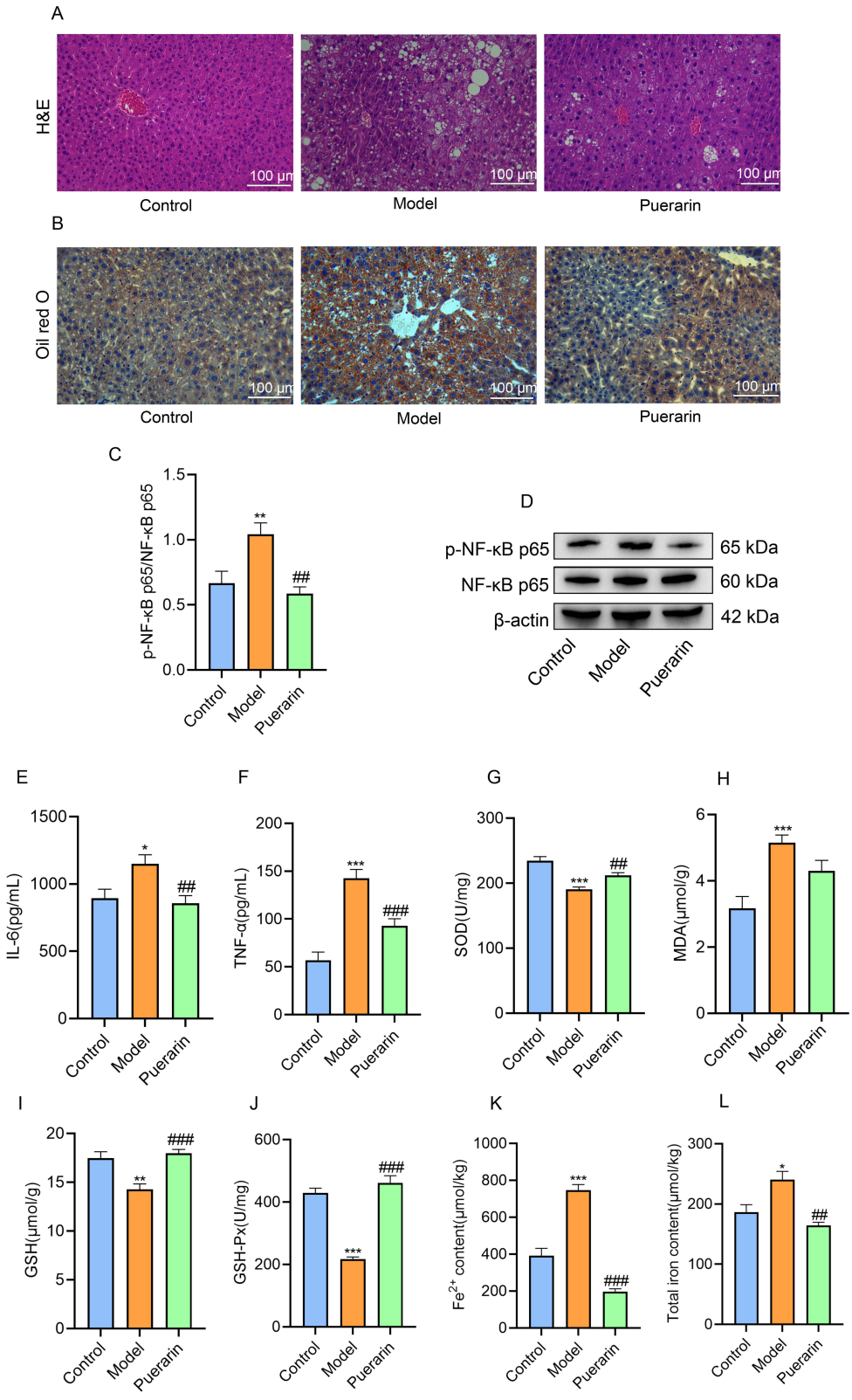

Figure 4 Effect of Puerarin on liver pathology, inflammatory reaction, oxidative stress, and iron overload in mice with DLI. (**A** and **B**) HE staining and Oil red O staining. Scale bar = 100 μm. (**C** and **D**) p-NF-κB p65 protein expression and Western blot bands. Data represent means ± SD (n = 5). (**E** and **F**) IL-6 and TNF-α levels in the liver. (**G-J**) SOD, MDA, GSH, and GSH-Px levels in the liver. (**K** and **L**) Fe^{2+} and total iron content in the liver. Data represent means ± SD (n = 8); Statistical analysis tested by one-way ANOVA test. $^{*}P < 0.05$, $^{**}P < 0.01$, $^{***}P < 0.001$ vs control; $^{\#\#}P < 0.01$, $^{\#\#\#}P < 0.001$ vs model.

https://doi.org/10.2147/DDDT.S487496

Effects of Puerarin on the Viability of AML12 Cells

To screen the time of HG stimulation, Western blotting was used to detect GPX4 protein expression level at different times of HG stimulation. The results showed that AML12 cells showed significant ferroptosis at 24 h of HG stimulation, and there was no significant difference between the expression level of GPX4 protein at 24 h and that at 36 h (Figure 5A and B). Therefore, 24 h was chosen as the time of HG stimulation. Besides, The CCK-8 assay was used to screen the appropriate administration concentration of Puerarin in vitro. AML12 cells were exposed to different concentrations of Puerarin for 24 h. 800 μM Puerarin had no effect on the viability of normal AML12 cells, suggesting that Puerarin is virtually non-pharmacotoxic (Figure 5C). AML12 cell viability was significantly inhibited under HG environment, and then AML12 cell viability was found to have a marked increase at 25, 50, and 100 μM, compared to the HG group (Figure 5D). Finally, 25, 50 and 100 μM were selected as the experimental drug concentrations.

Effects of Puerarin on Steatosis and Liver Function Indexes in HG-Induced AML12 Cells

Elevated levels of TC, TG, LDL-C, and reduced levels of HDL-C were observed in HG-stimulated AML12 cells, but the above indices were reversed by Puerarin treatment (Figure 5E-H). ALT and AST levels were elevated in the HG group compared to the control group, which indicated that the liver function of HG-stimulated AML12 cells was impaired. Then, liver function significantly improved when AML12 cells were treated with 25, 50 and 100 μM Puerarin (Figure 5I and J). Furthermore, Oil red O staining showed that significant lipid accumulation was observed in HG-induced AML12 cells, whereas lipid accumulation was reduced to varying degrees after 25, 50 and 100 μM Puerarin treatment (Figure 5K). These results confirmed the protective effect of Puerarin against HG-induced liver injury in AML12 cells.

Effects of Puerarin on JAK2/STAT3 Pathway and Ferroptosis in the Livers

In the present study, the specific mechanism by which Puerarin regulates ferroptosis to exert a protective effect was further explored. In this experiment, the expression of JAK2/STAT3 pathway-related proteins was detected by Western blotting. The results of mice experiments found that p-JAK2 and p-STAT3 protein expressions were markedly elevated in the livers of KKAy mice models, compared with the control group. The above indexes were significantly reduced after treatment with Puerarin (Figure 6A-C). To demonstrate that Puerarin modulates ferroptosis to ameliorate DLI, Western blotting was performed to detect the expression levels of ferroptosis-related indicators GPX4, ACSL4, PTGS2, SLC7A11, FTH1 and TFR1 proteins. The results showed that up-regulation of ACSL4, PTGS2, and TFR1 protein expression was observed in the livers of diabetic mice, in contrast to a decrease in the protein expression of GPX4, SLC7A11, and FTH1; the above indexes were reversed after Puerarin treatment (Figure 6D-J).

Effects of Puerarin on JAK2/STAT3 Pathway and Ferroptosis in the HG-Induced AML12 Cells

For AML12 cells, p-JAK2 and p-STAT3 protein expressions in HG-induced AML12 cells were remarkably higher than that in the control group, whereas 25, 50, and 100 μM Puerarin notably reduced p-JAK2 and p-STAT3 protein expressions in the HG group (Figure 7A-C). These results suggested that Puerarin inhibited the JAK2/STAT3 pathway in HG-induced AML12 cells. For AML12 cells, the results were consistent with in vivo experiments. Compared with the control group, HG-induced AML12 cells showed significant upregulation of ACSL4, PTGS2, and TFR1 protein expression, and noticeable decrease of GPX4, SLC7A11, and FTH1 expression; whereas the protein expression of the above indexes was restored to varying degrees after Puerarin intervention (Figure 7D-J). These data confirmed that Puerarin inhibited ferroptosis in HG-induced AML12 cells.

Effects of AG490 on Ferroptosis in HG-Induced AML12 Cells

To investigate the specific mechanism by which Puerarin inhibits ferroptosis to improve DLI, we used AG490 in vitro to explore the necessity of the JAK2/STAT3 pathway. Experimental data revealed that the HG+AG490 group obviously

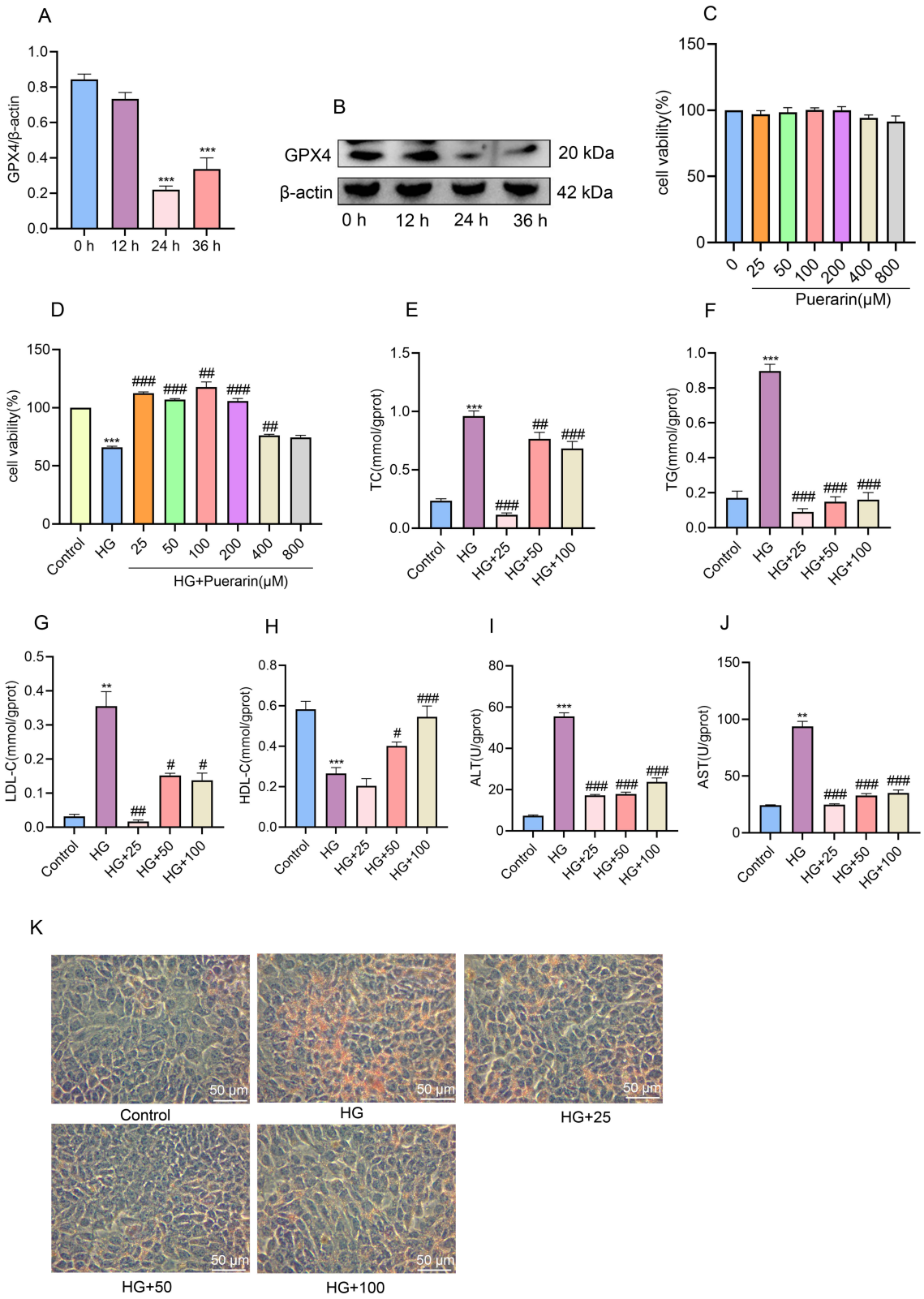

Figure 5 Effect of Puerarin on the viability, steatosis, and liver function indexes in HG-induced AML12 cells. (**A** and **B**) GPX4 protein expression and Western blot bands. Data represent means ± SD (n = 5). (**C** and **D**) CCK-8 assay of Puerarin on normal AML12 cells viability and HG-induced AML12 cells viability. Data represent means ± SD (n = 5). (**E-H**) TC, TG, LDL-C, and HDL-C levels in AML12 cells. (**I** and **J**) ALT and AST levels in AML12 cells. Data represent means ± SD (n = 5). (**K**) Oil red O staining of AML12 cells. Scale bar = 50 μm. Statistical analysis tested by one-way ANOVA test. $^{**}P < 0.01$, $^{***}P < 0.001$ vs control; $^{\#}P < 0.05$, $^{\#\#}P < 0.01$, $^{\#\#\#}P < 0.001$ vs HG.

https://doi.org/10.2147/DDDT.S487496

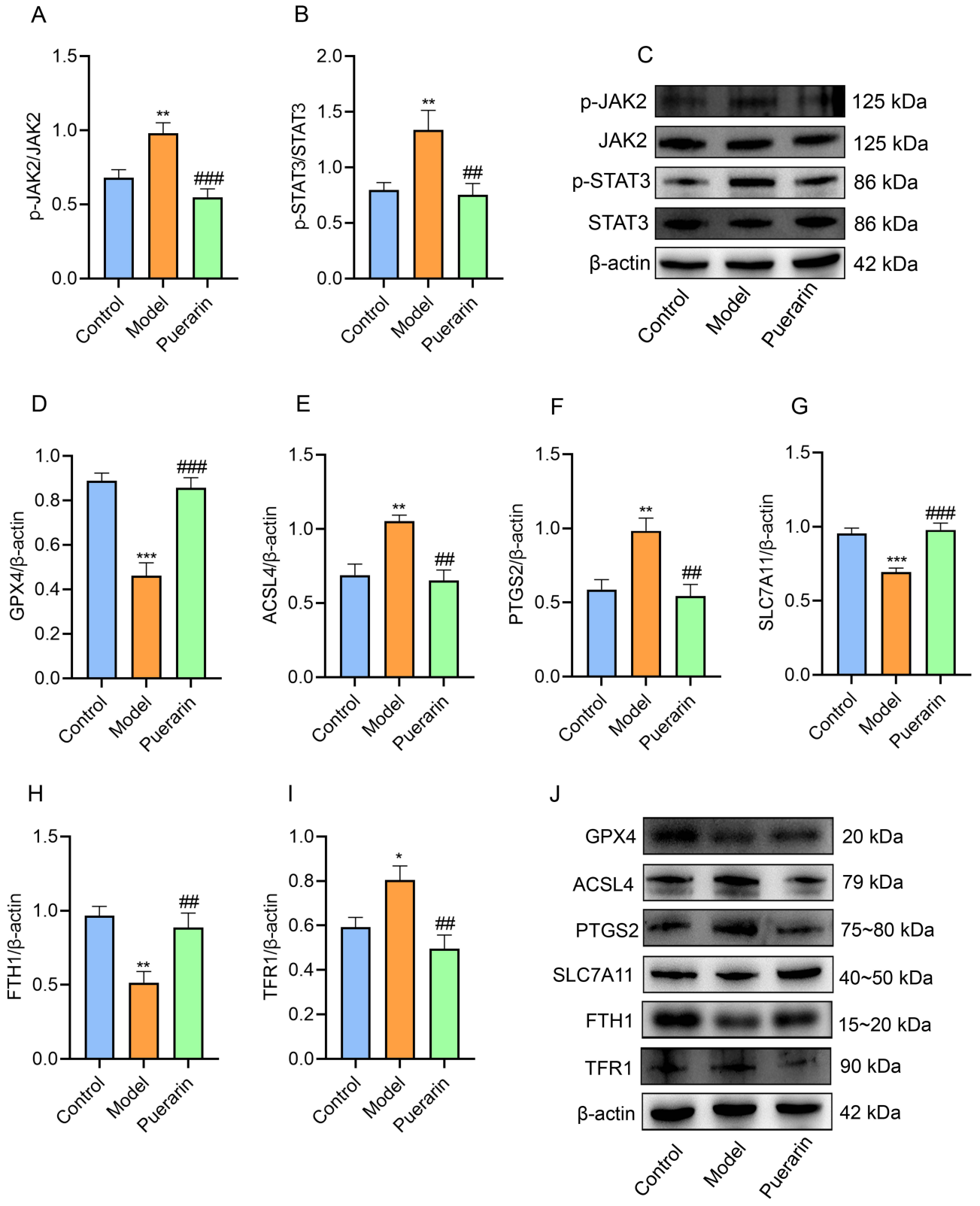

Figure 6 Effects of Puerarin on JAK2/STAT3 pathway and ferroptosis in mice with DLI. (**A-C**) p-JAK2 and p-STAT3 protein expression and the Western blot bands. (**D-J**) GPX4, ACSL4, PTGS2, SLC7A11, FTH1, and TFR1 protein expression and the Western blot bands. Data represent means ± SD (n = 5). Statistical analysis tested by one-way ANOVA test. $^{*}P < 0.05$, $^{**}P < 0.01$, $^{***}P < 0.001$ vs control; $^{\#\#}P < 0.01$, $^{\#\#\#}P < 0.001$ vs model.

https://doi.org/10.2147/DDDT.S487496

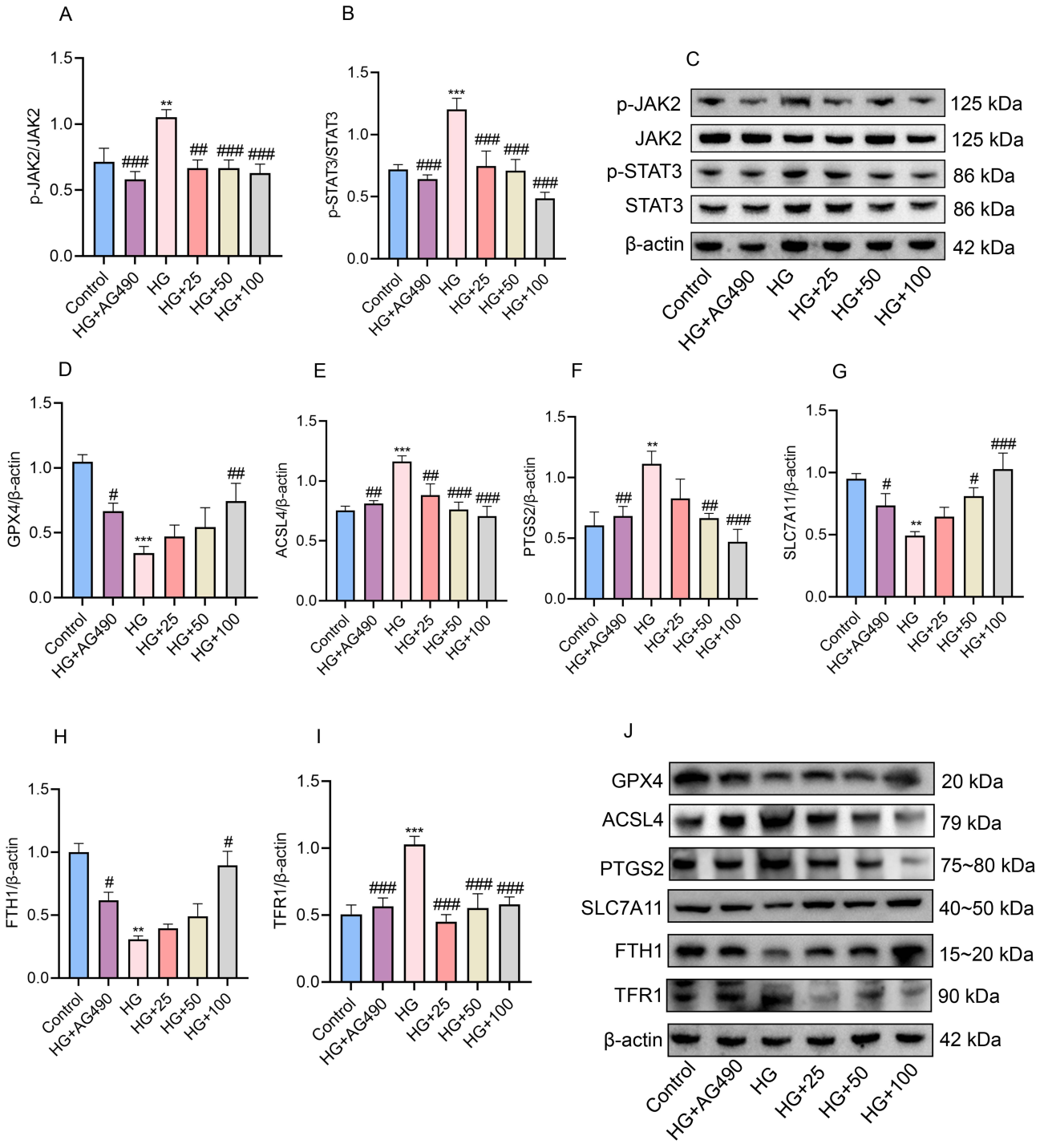

Figure 7 Effects of Puerarin and AG490 on JAK2/STAT3 pathway and ferroptosis in HG-induced AML12 cells. (**A-C**) p-JAK2 and p-STAT3 protein expression and the Western blot bands. (**D-J**) GPX4, ACSL4, PTGS2, SLC7A11, FTH1, and TFR1 protein expression and the Western blot bands. Data represent means ± SD (n = 5). Statistical analysis tested by one-way ANOVA test. $^{**}P < 0.01$, $^{***}P < 0.001$ vs control; $^{\#}P < 0.05$, $^{\#\#}P < 0.01$, $^{\#\#\#}P < 0.001$ vs model.

decreased the expression of p-JAK2 and p-STAT3 proteins in the HG group. The results also found that both HG+AG490 and HG+Puerarin (25, 50, and 100 μM) effectively improved ferroptosis-related indexes in the HG group to varying degrees, suggesting that AG490 and Puerarin exerted similar effects (Figure 7A-J). Finally, we conclude that the JAK2-STAT3 signaling pathway is involved in the improvement of ferroptosis in DLI by Puerarin.

https://doi.org/10.2147/DDDT.S487496

Discussion

Persistent hyperglycaemia and metabolic disorders in DM patients can cause systemic tissue and organ damage, which can lead to serious complications.[33] Among them, liver disease is the main cause of death in DM patients. Due to the complexity of the pathogenesis, there is no ideal specific drug or therapeutic strategy for the treatment of DLI. In this study, we aimed to investigate the effects and mechanisms of Pueraria in the treatment of DLI (Figure 8). In vivo, Puerarin inhibited the ferroptosis process in liver injury in KKAy mice through the JAK2/STAT3 pathway. In vitro, Puerarin ameliorated HG-induced liver injury in AML12 cells. Meanwhile, blocker experiments using AG490 confirmed that the inhibition of ferroptosis process by Puerarin was relied on the JAK2/STAT3 pathway. We believe that these findings collectively suggest that Puerarin is a promising and effective agent in the treatment of DLI.

The male KKAy mice selected for this study are type 2 diabetic mice with a mutation in the hair color gene (ie Ay). Ay gene causes metabolic disorders in mice, resulting in metabolic abnormalities syndromes such as hyperglycemia, obesity, and disorders of lipid metabolism.[34] The diabetes induced by this model is extremely similar to that of human type II diabetes, which makes it an ideal animal model of type II diabetes. The results of this experiment showed that the FBG, body weight, and lipid levels of KKAy mice on a high-sugar and high-fat diet were significantly higher than those of the control group, which proved that it was a stable animal model of type 2 diabetes. In addition, KKAy mice showed elevated ALT and AST levels as well as liver pathology with vacuoles, steatosis and lipid accumulation. All these results indicated that the DLI model was successfully constructed. However, all above indicators improved after administration of Puerarin, indicating that Puerarin effectively inhibited dyslipidaemia and protected liver structure and function in KKAy mice.

AML12 cells, mouse normal hepatocytes, were constructed from hepatocytes of transgenic mice carrying the human TGF-α gene. Easily grown AML12 cells were selected in this study due to difficulties in primary cell culture. Meanwhile, AML12 cells were cultured with HG in vitro to mimic the high-glucose microenvironment in diabetic hepatocytes.[35] This cell model has the advantages of high efficiency, short cycle time, good reproducibility and high operability, and has been widely used in the study of liver diseases caused by DM. Under HG intervention for 24 h, AML12 cell viability was obviously reduced and showed impaired liver function and steatosis, indicating that the vitro model was successfully

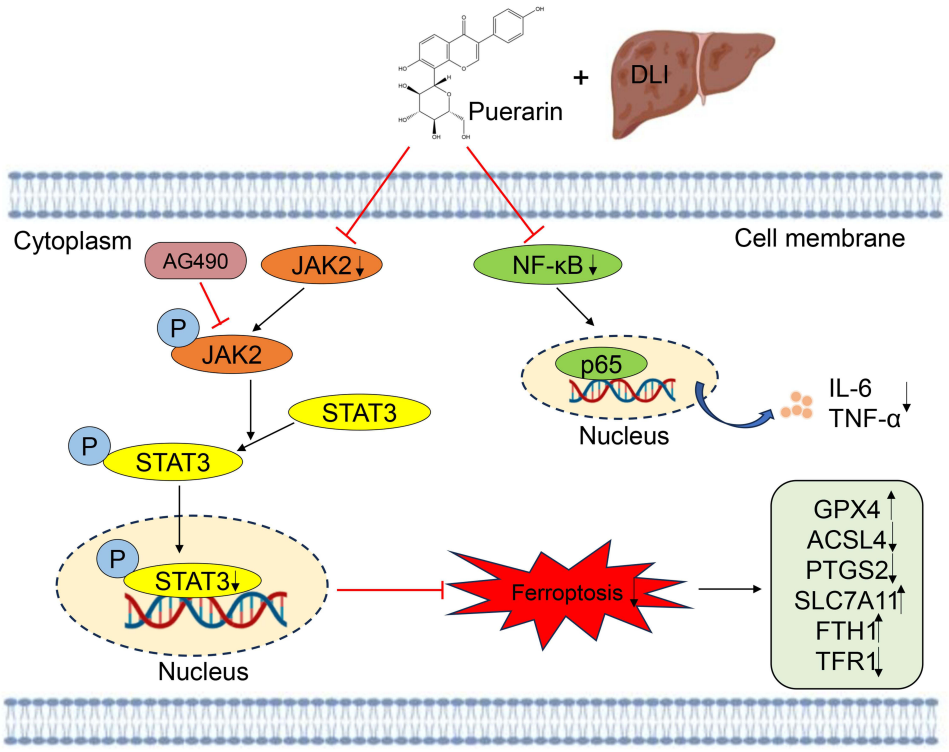

Figure 8 A schematic diagram illustrating the effects and mechanisms of Puerarin on DLI.

constructed. The above indexes were improved to varying degrees after the intervention with different concentrations of Puerarin, indicating that Puerarin has a protective effect on HG-induced liver injury in AML12 cells.

The present study investigated the effects of Puerarin on liver oxidative stress levels and iron homeostasis in diabetic mice. Lipid peroxidation and iron overload are critical for ferroptosis.[36] SOD, MDA, GSH, and GSH-Px are important intracellular indicators of redox status, which can comprehensively evaluate changes in oxidative stress levels.[37] During DLI, the liver is subjected to oxidative stress, with increased production of ROS, leading to a decrease in GSH content and the formation of lipid peroxides such as MDA. SOD, GSH and GSH-Px, the main intracellular antioxidants, scavenge free radicals and prevent lipid peroxidation reactions. In addition, the intracellular Fe^{2+} content increases and combines with H_2O_2 to generate hydroxyl radicals. Hydroxyl radicals oxidise polyunsaturated fatty acids on membranes, leading to lipid peroxidation.[38] When the intracellular antioxidant system is imbalanced, lipid peroxidation may be accelerated, causing cell membrane damage and ultimately inducing ferroptosis in cells. Our experimental results show that Puerarin can reduce iron content to a certain extent, as well as increase SOD, GSH, GSH-Px content and inhibit MDA production, thus alleviating the pathogenesis of DLI. Therefore, Fe, SOD, MDA, GSH, and GSH-Px can be used as important reflective indicators of the degree of oxidative stress damage and ferroptosis in DLI, which provides a new idea for the treatment of DLI with Puerarin by regulating redox balance and ferroptosis.

Ferroptosis is a unique mode of cell death associated with oxidative stress and disturbances in iron metabolism, which plays a key role in DLI.[39] Glutathione Peroxidase 4 (GPX4) is a negative regulator of lipid peroxidation and has an important role in preventing the development of ferroptosis.[40] GPX4, an antioxidant enzyme, reduces lipid peroxides to lipids alcohols with the assistance of glutathione (GSH). GSH depletion inactivates GPX4 and lipid peroxidation occurs, thereby inducing ferroptosis in cells.[41] Conversely, overexpression of GPX4 inhibits lipid accumulation, thereby protecting cells from oxidative damage. Besides, GSH, activated by the specific amino acid transport protein SLC7A11, is an vital cofactor in maintaining normal GPX4 function. Down-regulation of SLC7A11 resulted in reduced GSH synthesis and GPX4 inactivation, which ultimately caused cellular lipid peroxide accumulation and contributed to the development of ferroptosis.[42] Activation of the SLC7A11/GPX4 pathway was found to attenuate Cd-induced hepatotoxicity and ferroptosis in HepG2 cells.[43] Therefore, GPX4 and SLC7A11 are considered as key regulatory proteins to prevent cellular ferroptosis.[44]

Long-chain acyl-CoA synthetase 4 (ACSL4), a key enzyme in lipid metabolism, regulates the biosynthesis of various unsaturated fatty acids in cell membranes and plays a crucial role in processes such as apoptosis, lipid metabolism, and energy metabolism.[45] However, excessive upregulation of ACSL4 can increase lipid peroxidation, leading to enhanced cell membrane permeability and promoting ferroptosis in cells. It was found that knockdown of ACSL4 inhibited ferroptosis and inflammatory responses in I/R-AKI mice in vivo and erastin-induced ferroptosis in HepG2 and HL60 cells in vitro.[46] Therefore, ACSL4 is considered a positive regulator of ferroptosis.[47] In addition, PTGS2, also known as COX-2, is a key enzyme catalysing prostaglandin biosynthesis. During ferroptosis, upregulation of PTGS2 may lead to the accumulation of lipid peroxides, which in turn promotes ferroptosis.[48] Thus, changes in PTGS2 may affect the process of ferroptosis.

In this study, we also examined the expression of key mediators of iron metabolism, TFR1 and FTH1. TFR1 is a transmembrane glycoprotein that interacts with iron-binding transferrin and plays an important role in cellular iron uptake.[49] Fe^{3+} binds to transferrin (TF) on the cell membrane to form a complex, which is transported by TFR1 into the cell to be reduced to Fe^{2+}. After being transported by divalent metal ion transporter (DMT1), it leads to lipid peroxidation via the Fenton reaction, which ultimately causes ferroptosis.[50] TFR is required for ferroptosis, and TFR deficiency protects cells from ferroptosis.[51] Besides, ferritin heavy chain 1 (FTH1), an essential component of the human ferritin shell, regulates intracellular Fe^{2+} concentration by storing free Fe^{2+} and inhibits ferroptosis by reducing ROS production.[52] Thus, TFR1 and FTH1 play key roles in regulating cellular iron metabolism and maintaining iron homeostatic balance.

In this study, network pharmacology and molecular docking technology were used to find the common pathways of Puerarin, DLI and ferroptosis. Network pharmacology explores the complex relationship between the components and effects of traditional Chinese medicine (TCM) from the perspective of multi-targets and multi-pathways, which can elucidate the complex mechanism of action of TCM, and provide new technical support for drug research and

development, and drug therapy.[53] Meanwhile, molecular docking, as a computational method, can be used to simulate the interactions between drug molecules and targets and predict the binding modes and affinities of both.[54] Based on this, the intersecting targets of Puerarin, ferroptosis and DLI were obtained in this study, including ALB, HIF1A, STAT3, TP53, and JUN, suggesting that these targets may be the key targets of Puerarin in the treatment of DLI through the ferroptosis pathway. Through KEGG enrichment analysis, 105 pathways were screened, and those closely related to inflammation included JAK/STAT signaling pathway, AGE-RAGE signaling pathway, TNF signaling pathway, and MAPK signaling pathway. In addition, molecular docking preliminarily predicted that Puerarin has good affinity with JAK2 and STAT3. Therefore, our team continued to use in vivo and in vitro experiments to verify whether Puerarin acts on ferroptosis process via the JAK2/STAT3 pathway to treat DLI.

Increasing evidence suggests that inflammation is closely associated with diabetes-induced liver diseases.[55] NF-κB signaling, one of the important pathways in the inflammatory process, has been found to be associated with the pathogenesis of DLI. The NF-κB pathway has been reported to regulate the production of various pro-inflammatory cytokines. NF-κB can induce the expression of pro-inflammatory cytokines such as TNF-α and IL-1β.[56] In addition to this, the JAK2/STAT3 pathway, one of the important intracellular signaling pathways, plays a key role in the inflammatory response.[57] It has been demonstrated that over-activation of the JAK2/STAT3 pathway exists in most human liver diseases and animal models of liver injury. Activation of the JAK2/STAT3 pathway can cause an increase in the expression of inflammatory factors, leading to cellular inflammation and fibrosis, and ultimately accelerating the progression of DLI.[58] Inhibition of the JAK2/STAT3 pathway was found to ameliorate the inflammatory response in the liver of mice with high-fat diet-induced NAFLD.[59] Inactivation of the IL-6/JAK2/STAT3 pathway also exerted an anti-inflammatory effect on ConA-induced acute hepatitis in mice.[60] In addition, exposure to AFB1 activated the JAK2/STAT3/NLRP3 pathway thereby, leading to cellular pyroptosis and fibrosis in the liver.[61] In conclusion, the JAK2/STAT3 pathway has been shown to be one of the important pathogenic mechanisms in many inflammatory diseases. This is consistent with our experimental results that the JAK2/STAT3 pathway and NF-κB were activated in KKAy mice on a high-sugar and high-fat diet, yet administration of Puerarin exerted anti-inflammatory effects on DLI mice.

Inflammation is one of the pathogenic mechanisms of DLI. Recent evidence suggests that in the inflammatory microenvironment, ferroptosis and inflammatory pathways interact with each other and are jointly involved in the regulation of inflammatory processes.[62] Ferroptosis can influence inflammatory progression by modulating the activity of inflammatory signaling pathways. Meanwhile, in the inflammatory microenvironment, the secretion of relevant substances between microbes and host cells or between host cells can influence the ferroptosis process.[63] More importantly, inhibition of JAK/STAT3 pathway was found to reverse cell apoptosis and ferroptosis in cisplatin-induced acute kidney injury (CAKI) mice.[64] It was also found that JAK or STAT1 inhibition ameliorated ferroptosis in non-obese diabetic (NOD) mice modeled with Sjogren's syndrome (SS).[65] Thus, JAK/STAT pathway is closely related to ferroptosis.

In vitro, we used AG490 to elucidate the relationship between hepatic ferroptosis and the JAK2/STAT3 pathway. AG490, a specific inhibitor of JAK2, has been widely used in the study of the signaling and regulatory roles of JAK2. AG490 inhibits the autophosphorylation of the epidermal growth factor (EGF) receptor and inhibits DNA synthesis and cell proliferation.[66] Activation of the JAK2/STAT3 pathway was reported to exacerbate painful neuropathy in diabetic rats, and this pain was alleviated by 50 μM AG490.[31] Our experimental results also showed that AG490 inhibited the HG-induced JAK2/STAT3 pathway and ferroptosis in AML12 cells, supporting the conclusion that the protective effect of Puerarin-regulated ferroptosis process against DLI is dependent on the JAK2/STAT3 pathway.

Conclusion

In summary, our findings demonstrated that Puerarin has a protective effect against liver injury in KKAy mice and HG-induced AML12 cells, and its mechanism of action is related to the amelioration of ferroptosis by Puerarin via inhibition of the JAK2/STAT3 pathway. These results suggest that Puerarin is likely to be a promising drug for the treatment of DLI.

Abbreviations

DLI, Diabetic liver injury; DM, Diabetes mellitus; PPI, Protein-protein interaction; KEGG, Kyoto encyclopedia of genes and genomes; HG, High glucose; NAFLD, Non-alcoholic fatty liver disease; KKAy, KK/Upj-Ay/J; FBG, Fasting blood glucose; HbA1c, Hemoglobin A1c; GSP, Glycated serum protein; TC, Total cholesterol; TG, Triglyceride; LDL-C, Low-density lipoprotein cholesterol; HDL-C, High-density lipoprotein cholesterol; ALT, Alanine aminotransferase; AST, Aspartate aminotransferase; HE, hematoxylin-eosin; DMEM/F12, Dulbecco's modified eagle medium/nutrient mixture F-12; CCK-8, Cell counting kit-8; SDS-PAGE, Sodium dodecyl sulfate-polyacrylamide gel electrophoresis; NF-κB p65, Nuclear factor kappa-B p65; p-NF-κB p65, phospho-Nuclear factor kappa-B p65; JAK2, Janus tyrosine kinase 2; p-JAK2, phospho-Janus tyrosine kinase 2; STAT3, Signal transducer and activator of transcription 3; p-STAT3, phospho-Signal transducer and activator of transcription 3; GPX4, Glutathione peroxidase 4; ACSL4, Long-chain acyl-CoA synthetase 4; PTGS2, Prostaglandin-endoperoxide synthase 2; FTH1, Ferritin heavy chain 1; TFR1, Transferrin receptor 1; TCM, Traditional Chinese medicine; EGF, Epidermal growth factor; CAKI, cisplatin-induced acute kidney injury; NOD, non-obese diabetic; SS, Sjogren's syndrome.

Acknowledgments

All experiments were conducted at the Animal Experiment Centre and Research and Experimental Centre of Beijing University of Chinese Medicine. The authors are grateful to all participants of this experiment. Besides, authors are very grateful to the Research and Experimental Centre of Beijing University of Chinese Medicine for the guidance of the cell experiments. Some materials in Figures 3 and 8 are from biorender (https://www.biorender.com/).

Author Contributions

All authors made a significant contribution to the work reported, whether that is in the conception, study design, execution, acquisition of data, analysis and interpretation, or in all these areas; took part in drafting, revising or critically reviewing the article; gave final approval of the version to be published; have agreed on the journal to which the article has been submitted; and agree to be accountable for all aspects of the work.

Funding

This study was funded by the Key Special Project for Modernization of Traditional Chinese Medicine of the National Key Research and Development Program of China (2018YFC1706800).

Disclosure

All authors report no conflicts of interest in this work.

References

1. Bailey CJ, Day C. Treatment of type 2 diabetes: future approaches. *Br Med Bull*. 2018;126(1):123–137. doi:10.1093/brimed/ldy013
2. Thomas MC. The clustering of cardiovascular, renal, adipo-metabolic eye and liver disease with type 2 diabetes. *Metabolism*. 2022;128:154961. doi:10.1016/j.metabol.2021.154961
3. Bedi O, Aggarwal S, Trehanpati N, Ramakrishna G, Krishan P. Molecular and pathological events involved in the pathogenesis of diabetes-associated nonalcoholic fatty liver disease. *J Clin Exp Hepatol*. 2019;9(5):607–618. doi:10.1016/j.jceh.2018.10.004
4. Zhu H, Xiao Y, Guo H, et al. The isoflavone puerarin exerts anti-tumor activity in pancreatic ductal adenocarcinoma by suppressing mTOR-mediated glucose metabolism. *Aging (Albany NY)*. 2021;13(23):25089–25105. doi:10.18632/aging.203725
5. Zeng J, Zhao N, Yang J, et al. Puerarin induces molecular details of ferroptosis-associated anti-Inflammatory on RAW264.7 macrophages. *Metabolites*. 2022;12(7):653. doi:10.3390/metabo12070653
6. Zheng L, Xu H, Hu H, et al. Preparation, characterization and antioxidant activity of inclusion complex loaded with puerarin and corn peptide. *Food Bioscience*. 2022;49:101886. doi:10.1016/j.fbio.2022.101886
7. Zhou YX, Zhang H, Peng C. Effects of puerarin on the prevention and treatment of cardiovascular diseases. *Front Pharmacol*. 2021;12:771793. doi:10.3389/fphar.2021.771793
8. Yang F, Gao H, Niu Z, et al. Puerarin protects the fatty liver from ischemia-reperfusion injury by regulating the PI3K/AKT signaling pathway. *Braz J Med Biol Res*. 2024;57:e13229. doi:10.1590/1414-431X2024e13229.
9. Bai YL, Han LL, Qian JH, Wang HZ. Molecular mechanism of puerarin against diabetes and its complications. *Front Pharmacol*. 2021;12:780419. doi:10.3389/fphar.2021.780419

10. Zheng P, Ji G, Ma Z, et al. Therapeutic effect of puerarin on non-alcoholic rat fatty liver by improving leptin signal transduction through JAK2/STAT3 pathways. *Am J Chin Med*. 2009;37(1):69–83. doi:10.1142/S0192415X09006692
11. Meunier L, Larrey D. Chemotherapy-associated steatohepatitis. *Ann Hepatol*. 2020;19(6):597–601. doi:10.1016/j.aohep.2019.11.012
12. Kang OH, Kim SB, Mun SH, et al. Puerarin ameliorates hepatic steatosis by activating the PPARα and AMPK signaling pathways in hepatocytes. *Int J Mol Med*. 2015;35(3):803–809. doi:10.3892/ijmm.2015.2074
13. Liu Y, Qiu Y, Chen Q, Han X, Cai M, Hao L. Puerarin suppresses the hepatic gluconeogenesis via activation of PI3K/Akt signaling pathway in diabetic rats and HepG2 cells. *Biomed Pharmacother*. 2021;137:111325. doi:10.1016/j.biopha.2021.111325
14. Huang R, Wu J, Ma Y, Kang K. Molecular mechanisms of ferroptosis and its role in viral pathogenesis. *Viruses*. 2023;15(12):2373. doi:10.3390/v15122373
15. Pan Q, Luo Y, Xia Q, He K. Ferroptosis and liver fibrosis. *Int J Med Sci*. 2021;18(15):3361–3366. doi:10.7150/ijms.62903
16. Liu Q, Xu L, Ren G, Zhao J, Shao Y, Lu T. Supression Thioredoxin reductase 3 exacerbates the progression of liver cirrhosis via activation of ferroptosis pathway. *Life Sci*. 2023;321:121591. doi:10.1016/j.lfs.2023.121591
17. Liao H, Shi J, Wen K, et al. Molecular targets of ferroptosis in hepatocellular carcinoma. *J Hepatocell Carcinoma*. 2021;8:985–996. doi:10.2147/JHC.S325593
18. Moon MS, Richie JP, Isom HC. Iron potentiates Acetaminophen-induced oxidative stress and mitochondrial dysfunction in cultured mouse hepatocytes. *Toxicol Sci*. 2010;118(1):119–127. doi:10.1093/toxsci/kfq230
19. Jiang T, Xiao Y, Zhou J, et al. Arbutin alleviates fatty liver by inhibiting ferroptosis via FTO/SLC7A11 pathway. *Redox Biol*. 2023;68:102963. doi:10.1016/j.redox.2023.102963
20. Yang M, Xia L, Song J, et al. Puerarin ameliorates metabolic dysfunction-associated fatty liver disease by inhibiting ferroptosis and inflammation. *Lipids Health Dis*. 2023;22(1):202. doi:10.1186/s12944-023-01969-y
21. Liu B, Zhao C, Li H, Chen X, Ding Y, Xu S. Puerarin protects against heart failure induced by pressure overload through mitigation of ferroptosis. *Biochem Biophys Res Commun*. 2018;497(1):233–240. doi:10.1016/j.bbrc.2018.02.061
22. Li X, Wang Z, Zhang S, Yao Q, Chen W, Liu F. Ruxolitinib induces apoptosis of human colorectal cancer cells by downregulating the JAK1/2-STAT1-Mcl-1 axis. *Oncol Lett*. 2021;21(5):352. doi:10.3892/ol.2021.12613
23. Sun L, Yang Z, Zhang J, Wang J. Isoliquiritigenin attenuates acute renal injury through suppressing oxidative stress, fibrosis and JAK2/STAT3 pathway in streptozotocin-induced diabetic rats. *Bioengineered*. 2021;12(2):11188–11200. doi:10.1080/21655979.2021.2006978
24. Chen Y, Lu W, Jin Z, Yu J, Shi B. Carbenoxolone ameliorates hepatic lipid metabolism and inflammation in obese mice induced by high fat diet via regulating the JAK2/STAT3 signaling pathway. *Int Immunopharmacol*. 2019;74:105498. doi:10.1016/j.intimp.2019.03.011
25. Hu X, Li J, Fu M, Zhao X, Wang W. The JAK/STAT signaling pathway: from bench to clinic. *Signal Transduct Target Ther*. 2021;6(1):402. doi:10.1038/s41392-021-00791-1
26. Ma Z, Peng L, Sheng Y, Chu W, Fu Y. Anti-inflammatory effect of columbianadin against D-galactose-induced liver injury in vivo via the JAK2/STAT3 and JAK2/p38/NF-κB Pathways. *Pharmaceuticals (Basel)*. 2024;17(3):378. doi:10.3390/ph17030378
27. Li X, Liu J. FANCD2 inhibits ferroptosis by regulating the JAK2/STAT3 pathway in osteosarcoma. *BMC Cancer*. 2023;23(1):179. doi:10.1186/s12885-023-10626-7
28. Zhang N, Zheng Q, Wang Y, et al. Renoprotective effect of the recombinant anti-IL-6R fusion proteins by inhibiting JAK2/STAT3 signaling pathway in diabetic nephropathy. *Front Pharmacol*. 2021;12:681424. doi:10.3389/fphar.2021.681424
29. Liu J, Zhang Y, Cheng J, et al. Puerarin reduces the levels of AGE-modified proteins in serum and retinal tissues to improve the retinal damage in diabetic rats.
30. Wang A, Gong Y, Pei Z, Jiang L, Xia L, Wu Y. Paeoniflorin ameliorates diabetic liver injury by targeting the TXNIP-mediated NLRP3 inflammasome in db/db mice. *Int Immunopharmacol*. 2022;109:108792. doi:10.1016/j.intimp.2022.108792
31. Li CD, Zhao JY, Chen JL, et al. Mechanism of the JAK2/STAT3-CAV-1-NR2B signaling pathway in painful diabetic ne uropathy. *Endocrine*. 2019;64(1):55–66. doi:10.1007/s12020-019-01880-6
32. Song J, Tang Z, Li H, et al. Role of JAK2 in the pathogenesis of diabetic erectile dysfunction and an intervention with berberine. *J Sex Med*. 2019;16(11):1708–1720. doi:10.1016/j.jsxm.2019.08.014
33. Khan H, Khanam A, Khan AA, et al. The complex landscape of intracellular signalling in protein modification under hyperglycaemic stress leading to metabolic disorders. *Protein J*. 2024;43(3):425–436. doi:10.1007/s10930-024-10191-3
34. Yang ZH, Miyahara H, Takemura S, Hatanaka A. Dietary saury oil reduces hyperglycemia and hyperlipidemia in diabetic KKAy mice and in diet-induced obese C57BL/6J mice by altering gene expression. *Lipids*. 2011;46(5):425–434. doi:10.1007/s11745-011-3553-1
35. Jing FY, Weng YJ, Zhang YQ. The protective effect of sericin on AML12 cells exposed to oxidative stress damage in a high-glucose environment. *Antioxidants (Basel)*. 2022;11(4):712. doi:10.3390/antiox11040712
36. Wan J, Ren H, Wang J. Iron toxicity, lipid peroxidation and ferroptosis after intracerebral haemorrhage. *Stroke Vasc Neurol*. 2019;4(2):93–95. doi:10.1136/svn-2018-000205
37. Ahmed Amar SA, Eryilmaz R, Demir H, Aykan S, Demir C. Determination of oxidative stress levels and some antioxidant enzyme activities in prostate cancer. *Aging Male*. 2019;22(3):198–206. doi:10.1080/13685538.2018.1488955
38. Wu ZF, Liu XY, Deng NH, Ren Z, Jiang ZS. Outlook of FERROPTOSIS-TARGETED LIPID PEROXIDATION IN CARDIOVASCULAR DISEASE. *Curr Med Chem*. 2023;30(31):3550–3561. doi:10.2174/0929867330666221111162905
39. Stancic A, Velickovic K, Markelic M, et al. Involvement of ferroptosis in diabetes-induced liver pathology. *Int J mol Sci*. 2022;23(16):9309. doi:10.3390/ijms23169309
40. Zhang S, Zhang S, Wang H, Chen Y. Vitexin ameliorated diabetic nephropathy via suppressing GPX4-mediated ferroptosis. *Eur J Pharmacol*. 2023;951:175787. doi:10.1016/j.ejphar.2023.175787
41. Ursini F, Maiorino M. Lipid peroxidation and ferroptosis: the role of GSH and GPx4. *Free Radic Biol Med*. 2020;152:175–185. doi:10.1016/j.freeradbiomed.2020.02.027
42. Koppula P, Zhuang L, Gan B. Cystine transporter SLC7A11/xCT in cancer: ferroptosis, nutrient dependency, and cancer therapy. *Protein Cell*. 2021;12(8):599–620. doi:10.1007/s13238-020-00789-5
43. Zhang L, Shi WY, Xu JY, et al. Protective effects and mechanism of chemical- and plant-based selenocystine against cadmium-induced liver damage. *J Hazard Mater*. 2024;468:133812. doi:10.1016/j.jhazmat.2024.133812

44. Chen L, Qiao L, Bian Y, Sun X. GDF15 knockdown promotes erastin-induced ferroptosis by decreasing SLC7A11 expression. *Biochem Biophys Res Commun*. 2020;526(2):293–299. doi:10.1016/j.bbrc.2020.03.079
45. Doll S, Proneth B, Tyurina YY, et al. ACSL4 dictates ferroptosis sensitivity by shaping cellular lipid composition. *Nat Chem Biol*. 2017;13(1):91–98. doi:10.1038/nchembio.2239
46. Yuan H, Li X, Zhang X, Kang R, Tang D. Identification of ACSL4 as a biomarker and contributor of ferroptosis. *Biochem Biophys Res Commun*. 2016;478(3):1338–1343. doi:10.1016/j.bbrc.2016.08.124
47. Wang Y, Zhang M, Bi R, et al. ACSL4 deficiency confers protection against ferroptosis-mediated acute kidney injury. *Redox Biol*. 2022;51:102262. doi:10.1016/j.redox.2022.102262
48. Xu F, Zhang Z, Zhao Y, Zhou Y, Pei H, Bai L. Bioinformatic mining and validation of the effects of ferroptosis regulators on the prognosis and progression of pancreatic adenocarcinoma. *Gene*. 2021;795:145804. doi:10.1016/j.gene.2021.145804
49. Candelaria PV, Leoh LS, Penichet ML, Daniels-Wells TR. Antibodies targeting the transferrin receptor 1 (TfR1) as direct anti-cancer agents. *Front Immunol*. 2021;12:607692. doi:10.3389/fimmu.2021.607692
50. Nataraj A, Govindan S, Ramani P, et al. Antioxidant, anti-tumour, and anticoagulant activities of polysaccharide from calocybe indica (APK2). *Antioxidants (Basel)*. 2022;11(9):1694. doi:10.3390/antiox11091694
51. Gao M, Monian P, Quadri N, Ramasamy R, Jiang X. Glutaminolysis and Transferrin Regulate Ferroptosis. *Mol Cell*. 2015;59(2):298–308. doi:10.1016/j.molcel.2015.06.011
52. Cui S, Liu X, Liu Y, et al. Autophagosomes defeat ferroptosis by decreasing generation and increasing discharge of free Fe2+ in skin repair cells to accelerate diabetic wound healing. *Adv Sci (Weinh)*. 2023;10(25):e2300414. doi:10.1002/advs.202300414
53. Li X, Wu L, Liu W, et al. A network pharmacology study of Chinese medicine QiShenYiQi to reveal its underlying multi-compound, multi-target, multi-pathway mode of action. *PLoS One*. 2014;9(5):e95004. doi:10.1371/journal.pone.0095004
54. Huang SY, Zou X. Advances and challenges in protein-ligand docking. *Int J mol Sci*. 2010;11(8):3016–3034. doi:10.3390/ijms11083016
55. Amini M, Saboory E, Pourheydar B, Bagheri M, Naderi R. Involvement of endocannabinoid system, inflammation and apoptosis in diabetes induced liver injury: role of 5-HT3 receptor antagonist. *Int Immunopharmacol*. 2020;79:106158. doi:10.1016/j.intimp.2019.106158
56. Su CH, Lin CY, Tsai CH, et al. Betulin suppresses TNF-α and IL-1β production in osteoarthritis synovial fibroblasts by inhibiting the MEK/ERK/NF-κB pathway. *Journal of Functional Foods*. 2021;86:104729. doi:10.1016/j.jff.2021.104729
57. O'Shea JJ, Murray PJ. Cytokine signaling modules in inflammatory responses. *Immunity*. 2008;28(4):477–487. doi:10.1016/j.immuni.2008.03.002
58. Dodington DW, Desai HR, Woo M. JAK/STAT - emerging players in metabolism. *Trends Endocrinol Metab*. 2018;29(1):55–65. doi:10.1016/j.tem.2017.11.001
59. Yao J, Zhao Y. Lp-PLA2 silencing ameliorates inflammation and autophagy in nonalcoholic steatohepatitis through inhibiting the JAK2/STAT3 pathway. *PeerJ*. 2023;11:e15639. doi:10.7717/peerj.15639
60. Zhou Y, Chen J, Yao Z, Gu X. Gastrodin ameliorates Concanavalin A-induced acute hepatitis via the IL6/JAK2/STAT3 pathway. *Immunopharmacol Immunotoxicol*. 2022;44(6):925–934. doi:10.1080/08923973.2022.2093741
61. Cui Y, Wang Q, Zhang X, et al. Curcumin alleviates aflatoxin b1-induced liver pyroptosis and fibrosis by regulating the JAK2/NLRP3 Signaling pathway in ducks. *Foods*. 2023;12(5):1006. doi:10.3390/foods12051006
62. Dou J, Liu X, Yang L, Huang D, Tan X. Ferroptosis interaction with inflammatory microenvironments: mechanism, biology, and treatment. *Biomed Pharmacother*. 2022;155:113711. doi:10.1016/j.biopha.2022.113711
63. Deng L, He S, Guo N, Tian W, Zhang W, Luo L. Molecular mechanisms of ferroptosis and relevance to inflammation. *Inflamm Res*. 2023;72(2):281–299. doi:10.1007/s00011-022-01672-1
64. Dong XQ, Chu LK, Cao X, et al. Glutathione metabolism rewiring protects renal tubule cells against cisplatin-induced apoptosis and ferroptosis. *Redox Rep*. 2023;28(1):2152607. doi:10.1080/13510002.2022.2152607
65. Cao T, Zhou J, Liu Q, et al. Interferon-γ induces salivary gland epithelial cell ferroptosis in Sjogren's syndrome via JAK/STAT1-mediated inhibition of system Xc^-. *Free Radic Biol Med*. 2023;205:116–128. doi:10.1016/j.freeradbiomed.2023.05.027
66. Whigham CA, Hastie R, Hannan NJ, et al. Placental growth factor is negatively regulated by epidermal growth factor receptor (EGFR) signaling. *Placenta*. 2021;114:22–28. doi:10.1016/j.placenta.2021.08.002